


Research Article

Modelling Air Pollution Dynamics and Mitigation Strategies: A Mathematical Approach

M. Aakash¹, C. Gunasundari², S. Athithan³, G. Santhosh Kumar⁴, Mutum Zico Meetei^{5*}, Merdi Ahmed Orsud⁵

¹Department of Mathematics, Jeppiaar Engineering College, Jeppiaar Nagar, Chennai, 600119, India

²Department of Mathematics, College of Engineering, Anna University, Chennai, 600025, India

³Department of Mathematics, College of Engineering and Technology, SRM Institute of Science and Technology, Kattankulathur, 600203, India

⁴Department of Mathematics, Easwari Engineering College, Ramapuram, Chennai, 600089, India

⁵Department of Mathematics, College of Science, Jazan University, Jazan, 45142, Saudi Arabia
E-mail: mmeetei@jazanu.edu.sa

Received: 27 November 2024; **Revised:** 3 March 2025; **Accepted:** 7 March 2025

Abstract: In this paper, we explore the intricate dynamics of air pollution using a deterministic mathematical model. Our objective is to comprehensively analyse the factors that contribute to both pollution-free and endemic equilibria. The model, carefully designed, serves as a valuable tool for understanding air quality dynamics and its evolution over time. Here, we constructed a three-dimensional mathematical model, namely general air class $A(t)$, the polluted air class $P(t)$ and the class of clean air $C(t)$. The key focus of our investigation is the stability analysis of equilibrium points. Our model has two equilibrium points, pollution-free and endemic equilibrium. Specifically, we examine local asymptotic stability, identifying conditions on key parameters that determine the stability of both pollution-free and endemic equilibria. This analysis provides crucial insights into the resilience or vulnerability of the system under different conditions, offering a deeper understanding of the factors influencing air pollution dynamics. Also, we obtained a basic reproduction number for our model, using the next-generation matrix method. To further support the credibility and applicability of our conclusions, we verify our theoretical results through computing simulations, bridging the gap between mathematical abstraction and real-world scenarios.

Keywords: mathematical model, air pollution, stability, equilibrium points, routh-hurwitz criteria, basic reproduction number

MSC: 92B05, 34A08, 34A34

1. Introduction

A physical, biological and chemical alternation to the air in the atmosphere is called pollution. It is an act in which the waste materials and toxic substances harm our soil, air, water environment and space. And it is mostly caused by acts of human beings. So, controlling pollution in society is much more important to increase the life expectancy of living things. Many researchers contributed to mathematical modeling with distinct social issues like pollution, epidemics,

Biodiversity, etc. [1–4]. In this paper, we concentrate on air pollution. Air pollution is a type of environmental pollution that affects the air and is usually caused by smoke or other harmful gases, mainly oxides of carbon, Sulphur and nitrogen. Simply in other words, air pollution is the contamination of air due to the presence or introduction of a substance that has a poisonous effect. It is well known that air pollution can be harmful to our health [5]. It contains a mixture of solid particles, liquid droplets, and gases from a variety of sources such as industry, motor vehicles, heating appliances and natural events such as bushfires, windblown dust, pollen mold spores, etc. We all know that there are 2 types of air pollution namely, outdoor air pollution and indoor air pollution. Some of the major causes of air pollution are the burning of fossil fuels, agricultural activities (NH_3 , methane), exhaust from factories and industries (CO , hydrocarbons) which depletes the quality of air, mining operations (extraction of minerals from earth causes dust, air and health problem to workers), indoor air pollution (painting materials which kept in houses), volcanic eruption, dust storms and wildfires. In humans, it causes lung disease, dizziness, lung cancer, coughing, throat infection, headache, etc. Whereas in plants it causes damage to the trees, vegetables, fruits, and flowers, and sometimes the tree dies due to NH_3 , Cl , and H_2S , which brings acid rain due to air pollution. Simultaneously in animals, it causes skin infection, breathing problems, etc., and it affects the atmosphere by causing ozone layer decay, greenhouse effect, and global warming.

Recent research has extensively developed exposure models for certain air pollutants; however, multi-air-pollutant exposure models, particularly for particulate chemical species, remain underexplored in Asia. The absence of an integrated framework for assessing multi-air-pollutant exposure has limited comprehensive exposure and health impact evaluations. To address this gap, a study applied the Land-Use Regression (LUR) approach to estimate annual average exposure levels of multiple air pollutants in Hong Kong, a high-density and high-rise urban environment [6]. The model incorporated four key gaseous pollutants- PM_{10} , $\text{PM}_{2.5}$, NO_2 and O_3 along with four major PM_{10} chemical species. The proposed framework effectively accounted for 91%-97% of the variation in measured pollutant concentrations, with cross-validation R^2 values between 0.73 and 0.93. By utilizing this model, researchers generated high-resolution spatial distribution maps of pollutant concentrations, providing insights into weak-to-moderate spatial correlations between PM_{10} chemical species and key air pollutants. This distinction is valuable for evaluating independent chronic health effects and advancing air pollution exposure modeling. Another study introduced an efficient reduced-order modeling approach to examine urban air pollutant dispersion, emphasizing the need for real-time air quality monitoring due to increasing emissions linked to urbanization. The methodology involved solving a linear advection-diffusion problem using Reynolds-Averaged Navier-Stokes (RANS) equations for convective flow, with an empirical time series source term. While high computational demands often limit real-time applications, the study addressed this challenge by implementing a problem-specific methodology that integrates Proper Orthogonal Decomposition with Regression (POD-R) and Galerkin projection (POD-G) supported by the Discrete Empirical Interpolation Method (DEIM) [7]. Additionally, a feedforward neural network was employed to retrieve the reduced-order convective operator required for online evaluations. Validated through synthetic emissions and real wind measurements, the proposed approach significantly reduced computational costs, making it suitable for real-time air quality monitoring and reinforcing the potential of data-driven methodologies in large-scale environmental modeling.

Iveta Steinberger et al. have proposed the present study atmospheric model Operational Street Pollution Model (OPSM). It is used to calculate NO_x and PM_{10} concentration levels in the historical center (street canyon) of the city of Riga (Latvia) to minimize traffic-induced air pollution [8, 9]. Whereas in another paper (Pope CA III et al.) they proved that long-term exposure to fine particulate matter air pollution ($\text{PM}_{2.5}$) contributes to increased risk of mortality rate [10, 11]. According to the survey, the mortality rate due to air pollution in India is much higher when compared to global. i.e., $\frac{134}{100,000}$ people in India nearly $\frac{64}{100,000}$ people global (average). So, it is very much necessary to control the air pollution. We can somewhat control this air pollution by the use of public transport or bicycles, conserving energy (i.e., by switching off fans, AC, lights and TV when not in use), using paper bags (i.e., minimizing plastic bags) and avoiding smoking.

The rise of big data has enabled advanced models to predict air pollution trends across space and time. Traditionally, these models were evaluated using overall metrics that compare predictions to monitoring data. However, such methods do not effectively differentiate errors at timescales relevant for epidemiological studies, such as short-term variations affecting health assessments. A novel frequency-band model performance evaluation approach was introduced,

demonstrating improved accuracy in identifying acute errors that could bias short-term health effect studies. Simulations showed that this method produced lower Root Mean Square Error (RMSE) and higher correlation values compared to conventional approaches [12]. For instance, in $PM_{2.5}$ predictions in Salt Lake City, the frequency-band approach more effectively detected acute errors influencing short-term health associations. With an R^2 value of 0.95 compared to 0.57 from conventional approaches, this method enhances exposure model evaluation, ensuring reliability in epidemiological research. Advancements in air pollution modeling for large regions remain a priority for epidemiological studies. The integration of geostatistics and machine learning has provided new avenues for refining existing frameworks. Future developments are expected to incorporate spatial covariance models and enhance learning algorithms to improve exposure assessment accuracy. Additionally, urban air pollution poses a significant environmental health concern, particularly in metropolitan areas where pollutant concentrations are exacerbated by high-rise buildings and street canyon effects [13]. Existing data-driven models often fail to fully capture the intricate interactions between air pollution and urban dynamics. To address these limitations, a hybrid deep learning model, Deep-AIR, was developed, integrating a Convolutional Neural Network (CNN) with a Long Short-Term Memory (LSTM) network. This model enhances the learning of cross-feature spatial interactions, particularly road density, building height, and the street canyon effect. Applied in Hong Kong and Beijing, Deep-AIR outperformed baseline models, achieving accuracy rates of 67.6%, 77.2%, and 66.1% for fine-grained hourly estimations, 1-hour, and 24-hour air pollution forecasts in Hong Kong, and 65.0%, 75.3%, and 63.5% for Beijing. Saliency analysis further indicated that road density and the street canyon effect are the most significant predictors of NO_2 concentrations in Hong Kong, while meteorological conditions play a dominant role in $PM_{2.5}$ estimations [14]. These studies collectively highlight the importance of integrating novel methodologies, including data-driven modeling, machine learning, and computational optimization, to improve air pollution exposure assessments and real-time monitoring. Advancements in these areas will significantly enhance air quality prediction accuracy, benefiting both environmental research and public health policy development.

The main contribution of our study is the development of an Air Pollution Compartmental (APC) model that incorporates the dynamics of air pollution. The proposed model provides a structured mathematical framework to analyze the interactions between clean air, general air, and polluted air, offering insights into the factors influencing air pollution levels. Through equilibrium analysis, the study determines the conditions for pollution-free and endemic equilibria, while stability analysis examines the resilience of the system under different parameter settings. Numerical simulations validate the theoretical findings, enhancing the model's applicability in understanding and controlling air pollution. This research contributes to the broader field of environmental modeling by providing a novel approach to studying air pollution dynamics mathematically.

This paper is organized as follows. Section 2 presents the mathematical model. Section 3 is devoted to an examination of equilibria with basic reproduction numbers and Section 4 deals with stability analysis. Results from analyses are demonstrated by numerical simulations in Section 5. The paper ends with a brief discussion in Section 6 and in Section 7 provide the conclusion of our study.

2. The model formulation

We classify the entire air individuals $N(t)$ into three distinct categories: the general air class $A(t)$, the polluted air class $P(t)$, and the class of clean air $C(t)$. This categorization serves as a foundational structure for dissecting and analyzing the various states of air quality prevalent within the population. At the core of our model lies the fundamental assumption that the parameter β_1 embodies the process of air conditioning, explicitly representing the mechanism of air cleaning. This assumption posits that when polluted air, denoted as belonging to the class $P(t)$, undergoes a cleaning process, it transitions seamlessly into the clean air category, $C(t)$. This transition is not merely a theoretical construct but serves as a crucial aspect of our framework, capturing the dynamic interplay between pollution reduction efforts and improvements in air quality. By integrating this assumption, our model effectively encapsulates the transformative impact of interventions whether they be natural processes, technological advancements, or policy-driven actions on the overall cleanliness of the atmosphere. The linkage between β_1 and air purification underscores the direct influence of cleaning mechanisms on environmental

health, reinforcing the idea that strategic efforts aimed at reducing pollutants lead to tangible enhancements in air quality. This perspective allows us to quantify the efficiency of cleaning interventions and assess their broader implications in environmental management and public health.

Moreover, we introduce two additional parameters, β_2 and β_3 , to account for the rates at which cleanliness is lost within the clean air class $C(t)$. This dual parameterization highlights the dynamic and bidirectional nature of air quality maintenance and degradation. Specifically, the air within the clean air class $C(t)$ is subject to two competing processes: a portion may lose its cleanliness due to external factors such as contamination, emissions, or natural diffusion, thereby transitioning into the polluted air class $P(t)$, while another fraction may enter the general air class $A(t)$, representing a state that is neither actively polluted nor explicitly conditioned as clean. This framework acknowledges that air quality is not static but continuously influenced by environmental conditions, anthropogenic activities, and intervention efforts. The movement of air between these classes reflects the complex interactions governing atmospheric composition, where cleaning mechanisms, pollutant emissions, and natural dispersion collectively shape the distribution of air quality states over time. By incorporating this dynamic exchange, our model provides a more comprehensive representation of how air quality evolves in response to both degradation processes and remediation efforts. This intricate interplay between cleanliness, degradation, and the general air environment constitutes the core significance of our model. By the principles of simple mass action interactions, we present a concise yet comprehensive mathematical formulation that encapsulates these dynamic processes. Through this model, we aim to provide a versatile and insightful tool for studying the impact of cleaning interventions and the rates of cleanliness loss on the evolution of air quality within a population.

$$\begin{aligned}\frac{dA}{dt} &= \Lambda - \alpha AP + \beta_2 C - \mu A \\ \frac{dP}{dt} &= \alpha AP - \beta_1 P + \beta_3 C \\ \frac{dC}{dt} &= \beta_1 P - \beta_2 C - \beta_3 C\end{aligned}\tag{1}$$

Parameters description of the model model (1) is given in Table 1 and the switch plot of the system is described in Figure 1, which described the dynamics of air quality, specifically the interactions between general air, pollution, and clean air. The variable A represents general air, which is replenished at a rate Λ , but is also removed naturally at a rate μ and influenced by pollution through the interaction term αAP . Clean air C is introduced into the system via the cleaning process from pollution at a rate $\beta_1 P$, but can lose its cleanliness either by joining the general air at a rate β_2 or the polluted air at a rate β_3 . The pollution level P increases through the interaction between general air and pollution (αAP) and by the contribution of clean air turning polluted $\beta_3 C$, but it is reduced by the cleaning rate $\beta_1 P$. The model captures the delicate balance between the processes of air contamination, cleaning, and the dynamic exchanges between these three components, offering insight into how pollution can accumulate or be mitigated based on the rates of these interactions.

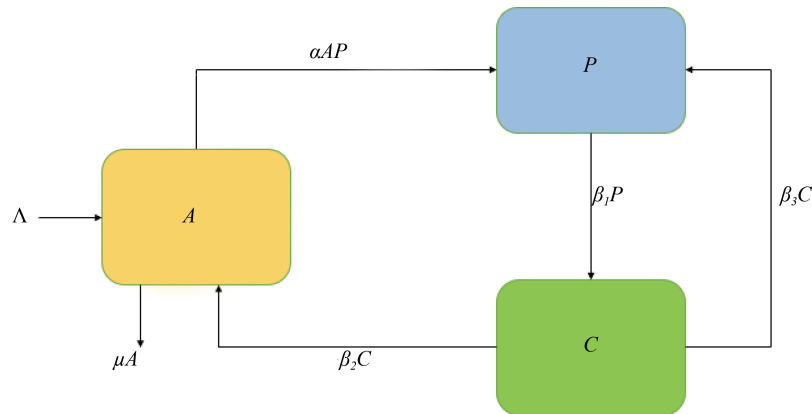


Figure 1. Switch plot of the system (1)

Table 1. Summary of factors

Factors	A detailed review
Λ	Recruitment rate
μ	Natural air removal rate from one place to another place
α	Interaction rate between general air with pollution
β_1	Conditioning or cleaning air
β_2	Rate of losing the cleanliness and joins general air
β_3	Rate of losing the cleanliness and joins polluted air

2.1 Positivity

Theorem 1 The problem of the system (1) provides a positive result.

Proof 1 From Equation (1) we have,

$$\left[\frac{dA}{dt} \right]_{A=0} = \Lambda + \beta_2 C \geq 0,$$

$$\left[\frac{dP}{dt} \right]_{P=0} = \beta_3 C \geq 0,$$

$$\left[\frac{dC}{dt} \right]_{C=0} = \beta_1 P \geq 0.$$

The result makes it very apparent that every parameter and population is positive. All of the solutions to our model (1) are therefore guaranteed to be non-negativity. Hence, the proof.

2.2 Boundedness

Theorem 2 The results of our model (1) are limited in feasible region R^3 .

Proof 2 From (1), the entire population size $N = A + P + C$ and the rate of change of N is given by,

$$\frac{dN}{dt} = \frac{dA}{dt} + \frac{dP}{dt} + \frac{dC}{dt},$$

For $\gamma > 0$,

$$\frac{dN}{dt} + \Upsilon N = \frac{dA}{dt} + \frac{dP}{dt} + \frac{dC}{dt} + \Upsilon N.$$

Once we integrate our model (1) into the above-mentioned equation, we get the following outcomes,

$$\frac{dN}{dt} + \Upsilon N \leq \Lambda - \alpha AP + \beta_2 C - \mu A + \alpha AP - \beta_1 P + \beta_3 C + \beta_1 P - \beta_2 C - \beta_3 C + \Upsilon N$$

$$\leq \Lambda - \mu A + \Upsilon N,$$

$$\leq \Lambda$$

After solving, we obtain

$$N(t) \leq \frac{\Lambda}{\Upsilon} \left(1 - e^{-\Upsilon t} \right) + N(0)e^{-\Upsilon t}, \text{ for } t \rightarrow \infty, N(t) \rightarrow \frac{\Lambda}{\Upsilon}.$$

As all the solutions of A , P , C are positive, we have

$$0 \leq N(t) \leq \frac{\Lambda}{\Upsilon}.$$

Thus, the space that seems feasible for the model (1) is given by a positive invariant set:

$$\Omega = \left\{ (A, P, C) \in R_+^3 : 0 \leq N(t) \leq \frac{\Lambda}{\Upsilon} \right\}$$

Therefore, the proof.

3. Equilibrium analysis and basic reproduction number

The equilibria for our model are determined by setting right hand sides of the model (1) to zero. The equilibria of the system (1) are denoted by $E_0 = (A^0, P^0, C^0)$ and $E_1 = (A^*, P^*, C^*)$.

3.1 Pollution Free Equilibrium (PFE)

For the system (1) it is easy to note that the free equilibrium is $E_0 = (A^0, P^0, C^0) = \left(\frac{\Lambda}{\mu}, 0, 0 \right)$.

3.2 Endemic Equilibrium (EE)

For the system (1) it is easy to note that the endemic equilibrium is $E_1 = (A^*, P^*, C^*)$. Here,

$$A^* = \frac{\Lambda\alpha\beta_2k_1 - \Lambda\beta_1\alpha + \Lambda\beta_3k_1\alpha - \beta_2k_1\alpha\Lambda + \beta_2k_1\beta_1\mu - \beta_2k_1^2\beta_3\mu}{\mu\alpha\beta_2k_1 - \mu\beta_1\alpha + \mu\beta_3k_1\alpha - \alpha^2\Lambda + \alpha\beta_1\mu - \alpha\beta_3k_1\mu}$$

$$P^* = \frac{-\alpha\Lambda - \beta_3k_1\mu + \beta_1\mu}{\alpha\beta_2k_1 - \beta_1\alpha + \beta_3k_1\alpha}$$

$$C^* = \frac{-\alpha\Lambda k_1 - \beta_3k_1^2\mu + \beta_1\mu k_1}{\alpha\beta_2k_1 - \beta_1\alpha + \beta_3k_1\alpha}$$

where, $k_1 = \frac{\beta_1}{\beta_2 + \beta_3}$.

3.3 Basic reproduction number

The basic reproduction number (R_0) is a crucial epidemiological parameter used to quantify the transmission potential of an infectious disease within a population. It is defined as the expected number of secondary infections produced by a typical infected individual in a fully susceptible population during the entire duration of their infectious period. In other words, R_0 provides an estimate of the average number of new infections that can arise from a single infected individual in a population where everyone is initially susceptible. To calculate R_0 , a mathematical model is employed, and in this context, the method described in reference [15] is utilized for our formulated APC model. The notation and approach outlined in [15] serve as the foundation for the subsequent computations. The matrices F and V play a pivotal role in this calculation. These matrices encapsulate essential information about the dynamics of the air pollution within the compartment. Specifically, F and V are defined as follows:

$$\mathfrak{F} = \begin{pmatrix} 0 \\ \alpha AP \\ 0 \end{pmatrix}, \quad v = \begin{pmatrix} -\Lambda + \alpha AP - \beta_2 C + \mu A \\ \beta_1 P - \beta_3 C \\ -\beta_1 P + \beta_2 C + \beta_3 C \end{pmatrix}.$$

The computation of R_0 involves analyzing the eigenvalues of the next-generation matrix, which is typically derived from the product of the matrices F and V . Thus, the basic reproduction number R_0 where the following is the matrix's electromagnetic range.

FV^{-1} is given by,

$$R_0 = \frac{\Lambda\alpha(\beta_2 + \beta_3)}{(\mu(-\beta_1\beta_3 + \beta_1(\beta_2 + \beta_3)))}.$$

Here the reproduction number R_0 gives the average number of polluted Air generated in a fully general air compartment.

3.4 Policy measures to reduce basic reproduction number

To reduce basic reproduction number, we need to do the following,

- A. Reducing pollution recruitment (Λ)
 - a. Implementing stricter emission regulations for industries and vehicles.
 - b. Encouraging the use of renewable energy sources.
 - c. Reducing industrial and agricultural pollutants at the source.
- B. Decreasing the interaction rate between general air and pollutants (α)
 - a. Implementing better waste management to prevent pollutant dispersion.
 - b. Increasing green spaces to absorb pollutants naturally.
- C. Enhancing air cleaning mechanisms (β_1)
 - a. Investing in advanced air filtration and purification technologies.
 - b. Promoting indoor and outdoor air purification systems.
 - c. Increasing forestation efforts to naturally filter air.
- D. Reducing the rate of clean air becoming polluted (β_2, β_3)
 - a. Reducing deforestation to maintain clean air balance.
 - b. Implementing policies to prevent recontamination of cleaned air.
- E. Improving natural airflow and ventilation (μ)
 - a. Designing urban areas to promote better air circulation.
 - b. Encouraging natural and mechanical ventilation in high-pollution zones.

By implementing these policies, pollution levels can be reduced effectively, leading to cleaner air and better public health outcomes.

4. Stability analysis

The Jacobi matrix for the system (1) is given by

$$J = \begin{pmatrix} -\alpha P - \mu & -\alpha A & \beta_2 \\ \alpha P & \alpha A - \beta_1 & \beta_3 \\ 0 & \beta_1 & -\beta_2 - \beta_3 \end{pmatrix}$$

4.1 Local stability analysis of PFE point

Theorem 3 Pollution free equilibrium E_0 is locally systematically stable if $R_0 < 1$ and otherwise it is not stable.

Proof 3 To study the stability of Pollution-Free Equilibrium (PFE), the variational matrix J_0 of the system evaluated at the PFE is obtained as,

$$J_0 = \begin{pmatrix} -\mu & -\frac{\alpha\Lambda}{\mu} & \beta_2 \\ 0 & \frac{\alpha\Lambda}{\mu} - \beta_1 & \beta_3 \\ 0 & \beta_1 & -\beta_2 - \beta_3 \end{pmatrix}$$

It is clearly found that one of the eigenvalues of the matrix J_0 is $-\mu_1$. The matrix of values is used to determine the other two value ranges, $\begin{pmatrix} \frac{\alpha\Lambda}{\mu} - \beta_1 & \beta_3 \\ \beta_1 & -\beta_2 - \beta_3 \end{pmatrix}$. By Routh-Hurwitz criteria the Pollution free equilibrium E_0 is locally asymptotically stable when $a_1 > 0$, $a_2 > 0$. Here, $a_1 = -\left(\frac{\alpha\Lambda}{\mu} - \beta_1 - \beta_2 - \beta_3\right)$ and $a_2 = -\frac{\alpha\Lambda\beta_3}{\mu} - \frac{\alpha\Lambda\beta_3}{\mu} + \beta_1\beta_2$. So,

a_1 is greater than zero only if it satisfies $-\frac{\alpha\Lambda\beta_2}{\mu} - \frac{\alpha\Lambda\beta_3}{\mu} < \beta_1\beta_2$, provided $R_0 < 1$. Hence the Pollution Free Equilibrium E_0 is locally asymptotically stable when $R_0 < 1$. Hence the theorem.

Theorem 4 E_I is locally asymptotically stable if $b_1 > 0$, $b_2 > 0$, $b_1 \cdot b_2 > b_3$ and otherwise it is said to be unstable.

Proof 4 The variational matrix, J_1 corresponding to the EE point E_1 is given by

$$J_1 = \begin{pmatrix} -\alpha P^* - \mu & -\alpha A^* & \beta_2 \\ \alpha P^* & \alpha A^* - \beta_1 & \beta_3 \\ 0 & \beta_1 & -\beta_2 - \beta_3 \end{pmatrix}$$

By Routh-Hurwitz criteria the endemic equilibrium E_1 is locally asymptotically stable when $b_1 > 0$, $b_3 > 0$ and $b_1 \cdot b_2 > b_3$. The characteristic polynomial of this matrix is given by,

$$\Lambda^3 + b_1\Lambda^2 + b_2\Lambda + b_3 \quad (2)$$

Here,

$$b_1 = -[n_{11} + n_{22} + n_{33}],$$

$$b_2 = [n_{22}n_{33} - n_{32}n_{23} + n_{11}n_{33} - n_{31}n_{13} + n_{11}n_{22} - n_{21}n_{12}],$$

$$b_3 = -|B|.$$

By Solving this we get,

$$b_1 = \alpha P^* + \mu + \beta_1 + \beta_2 + \beta_3 - \alpha A^*,$$

$$b_2 = \alpha A^* (-\beta_2 - \beta_3 - \mu) + \alpha P^* (\beta_1 + \beta_2 + \beta_3) + \mu(\beta_1 + \beta_2 + \beta_3) + \beta_1\beta_2$$

and

$$b_3 = \alpha P^* \beta_1 \beta_3 (\alpha P^* + \alpha \mu + 1 + \mu) + \mu \beta_1 (\beta_2 + \beta_3 + \mu \beta_3) - \alpha A^* \mu (\beta_2 + \beta_3)$$

Here, b_1 is greater than zero only if $-\alpha A^* < \alpha P^* + \mu + \beta_1 + \beta_2 + \beta_3$, b_2 is only positive if $\alpha A^* (\beta_2 - \beta_3 - \mu) < \alpha P^* (\beta_1 + \beta_2 + \beta_3) + \mu (\beta_1 + \beta_2 + \beta_3) + \beta_1\beta_2$ and b_3 is only positive if $-\alpha A^* \mu (\beta_2 + \beta_3) < \alpha P^* \beta_1 \beta_3 (\alpha P^* + \alpha \mu + 1 + \mu) + \mu \beta_1 (\beta_2 + \beta_3 + \mu \beta_3)$.

Now clearly, when $b_1 > 0$, $b_3 > 0$ and $b_1 \cdot b_2 > b_3$ provided $R_0 > 1$. Hence the Endemic Equilibrium E_1 is locally asymptotically stable when $R_0 > 1$.

4.2 Global stability analysis of PFE pointc

Theorem 5 The region's ecological equilibrium is steady globally Ω .

Proof 5 To establish the global stability of the region Ω , we focus our analysis on the A and P equations, excluding the compartment C . This reduction allows for a simplified examination of the dynamics within the general air class and polluted air class. Within the first quadrant of the A, P plane, we employ Dulac's criteria with the chosen multiplier $D = \frac{1}{P}$. Since, Dulac's criteria is a mathematical tool used to assess the existence of limit cycles in dynamical systems. The application of Dulac's criteria is aimed at revealing information about the stability of the system and whether trajectories within the AP plane tend to converge towards equilibrium points or exhibit other complex behaviours. So, by focusing on the general air and polluted compartments, we gain insights into the global stability properties of the region Ω under consideration. Reference [16] likely provides further details or context for the specific model or system being analyzed, and consulting this source may offer additional insights into the mathematical and theoretical aspects of the stability analysis [17, 18].

We consider

$$F_1 = \Lambda - \alpha AP - \mu A,$$

$$F_2 = \alpha AP - \beta_1 P.$$

Applying Dulac's criteria, we have

$$DF_1 = \frac{\Lambda}{P} - \alpha A - \frac{\mu A}{P},$$

$$DF_2 = \alpha A - \beta_1.$$

Now we have,

$$\frac{\partial (DF_1)}{\partial A} + \frac{\partial (DF_2)}{\partial P} = -\alpha - \frac{\mu}{P}.$$

From the above condition, it can be noted that the region Ω lacks a periodic solution. For any solution initiating in the quadrant that is positive of the AP plane, where P is greater than zero and $A + P \leq \frac{\Lambda}{\beta_1}$, the trajectory converges towards (A^*, P^*) as time t tends towards infinity. This convergence is evident in the behaviour of the system described by the equations in (1), where C approaches C^* . Consequently, the point (A^*, P^*, C^*) attains global stability within the region Ω .

5. Numerical simulation

The system (1) is subjected to simulations across diverse parameter sets that adhere to the conditions ensuring the local asymptotic stability of equilibria E_0 and E_1 . In Figure 2, the stability of the pollution-free equilibrium E_0 is demonstrated for a specific set of parameter values, $\Lambda = 10$; $\alpha = 0.00049$; $\beta_1 = 0.51$; $\beta_2 = 0.08$; $\beta_3 = 0.001$; $\mu = 0.014$. In this context, the calculated basic reproduction number is denoted as $R_0 = 0.0096$. In Figure 3, the stability of the endemic equilibrium

point E_1 is illustrated for another set of parameter values, $\Lambda = 10$; $\alpha = 0.00049$; $\beta_1 = 0.51$; $\beta_2 = 0.92$; $\beta_3 = 0.001$; $\mu = 0.14$. For this particular parameter set, the associated reproduction number is computed as $R_0 = 2.9485$. These simulations and parameter variations provide valuable insights into the stability characteristics of both the pollution-free equilibrium E_0 and the endemic equilibrium E_1 within the given system.

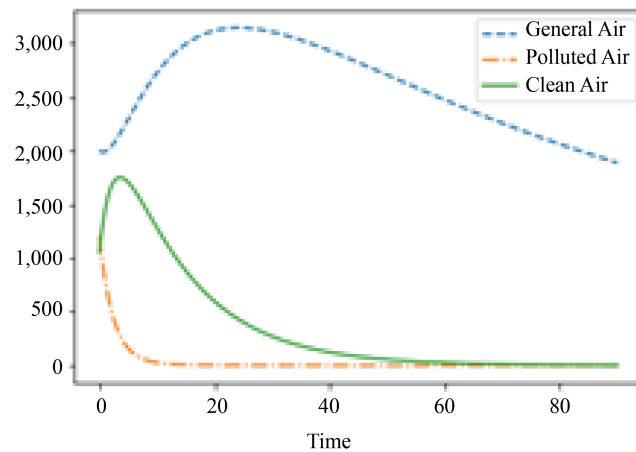


Figure 2. Variation of A, P, C with time for pollution free equilibrium of (1)

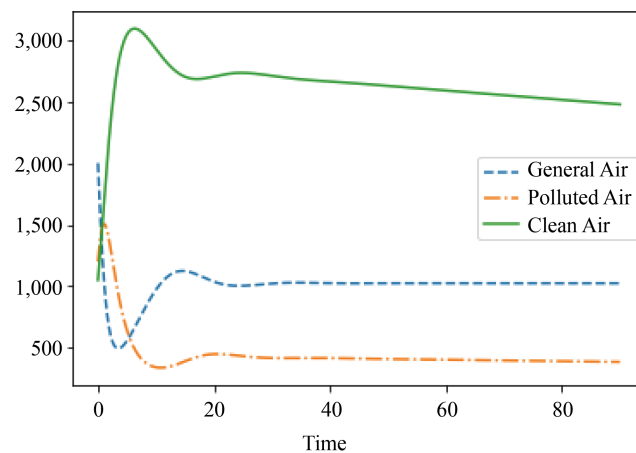


Figure 3. Configuration of A, P, C with time for endemic equilibrium of (1)

Figure 4 depicts a 3D phase portrait. The phase portrait represents the behavior of a system of differential equations over time in a graphic form. This diagram illustrates the trajectory of the state variables of the system in state space. As shown in the Figure 4, the phase portrait shows 10 random initial conditions. The text labels next to the curves indicate the specific initial conditions used to generate the trajectory. For instance, the red curve corresponds to the initial conditions $[5.62, 14.26, 10.98]$. The axes of the 3D phase portrait are designated $M[0]$, $M[1]$, and $M[2]$. We hypothesize that these variables correspond to the mass fractions of general air, polluted air, and clean air, respectively, within the modeled system. These state variables evolve over time as the system progresses, and the trajectories depict this evolution. Therefore, the phase portrait serves as a visualization of the dynamical system's behavior for ten distinct initial mass fractional compositions.

3D Phase Portraits with 10 Random Initial Conditions

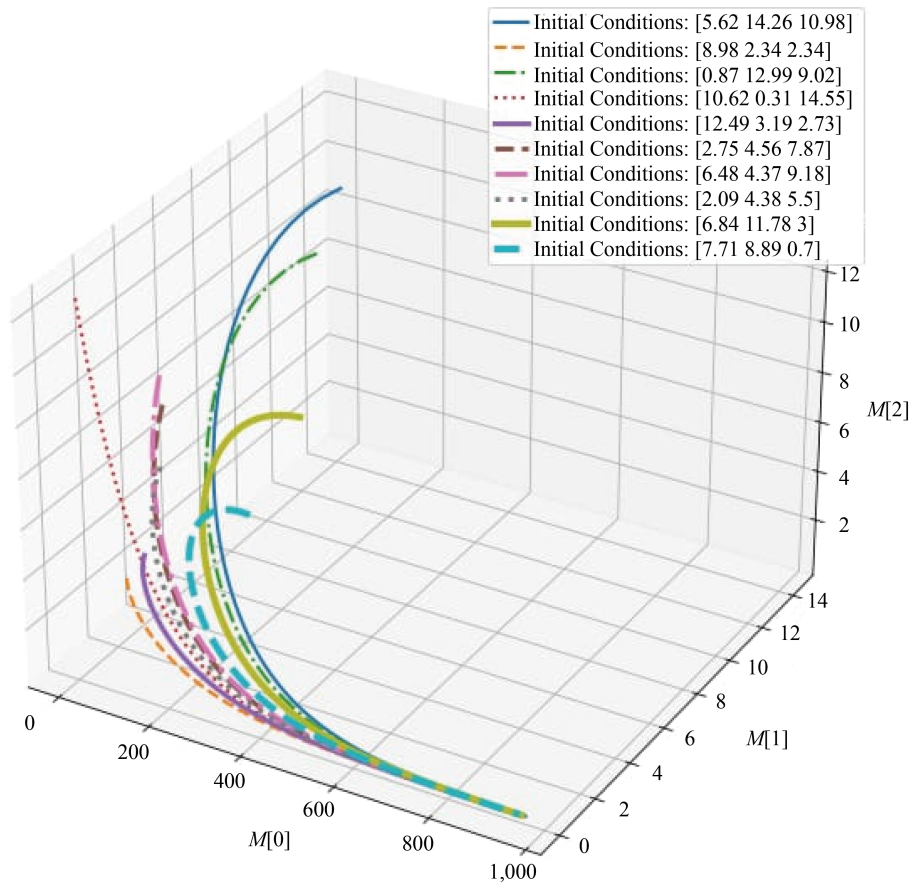


Figure 4. 3D phase portrait representation of the initial conditions for the solutions of system (1)

Figure 5 demonstrates the phase portraits for system (1), which are used to visualize the behavior of solutions to a system of differential equations. Trajectories are depicted in the portrait, which are the paths taken by solutions over time. This plot shows that the solutions of (1) converge to three distinct points over the period 't'. The blue curve represents the competition between the general air and the polluted air population. The orange curve represents the competition between polluted and clean air among the population. And, the green curve depicts the trajectory between general air and clean air class. These three curves correlate at a particular point (1,000, 1,000) in the phase plane plot for the solutions of the system (1).

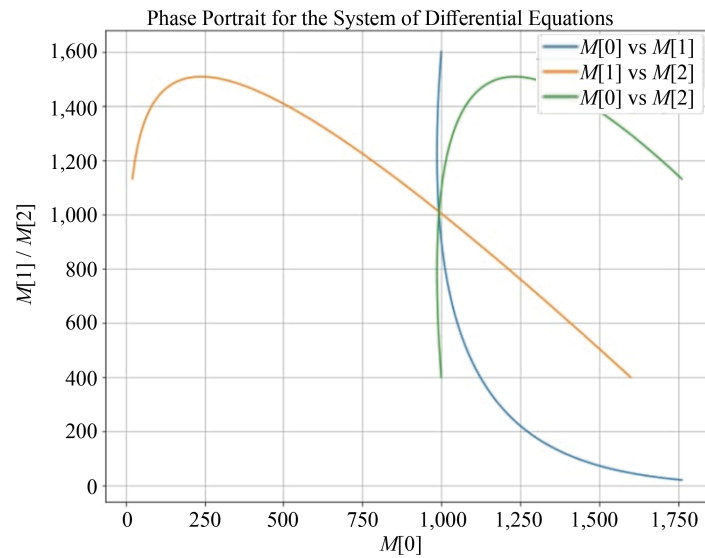


Figure 5. Phase portrait plot between general, polluted and cleaned air classes

Figure 6 depicts contour plots representing the dynamics of a system of differential equations in a two-dimensional space. This space serves as a representation of the initial conditions for the system under study. Specifically, Figure 6a illustrates the contour plot analyzing the interplay between the recruitment rate Λ and the interaction rate between unpolluted air and polluted air α . On the other hand, Figure 6b showcases the contour plot exploring the relationship between the recruitment rate Λ and the rate at which cleanliness is lost, leading to contamination β_3 . Meanwhile, Figure 6c presents the contour plot c .

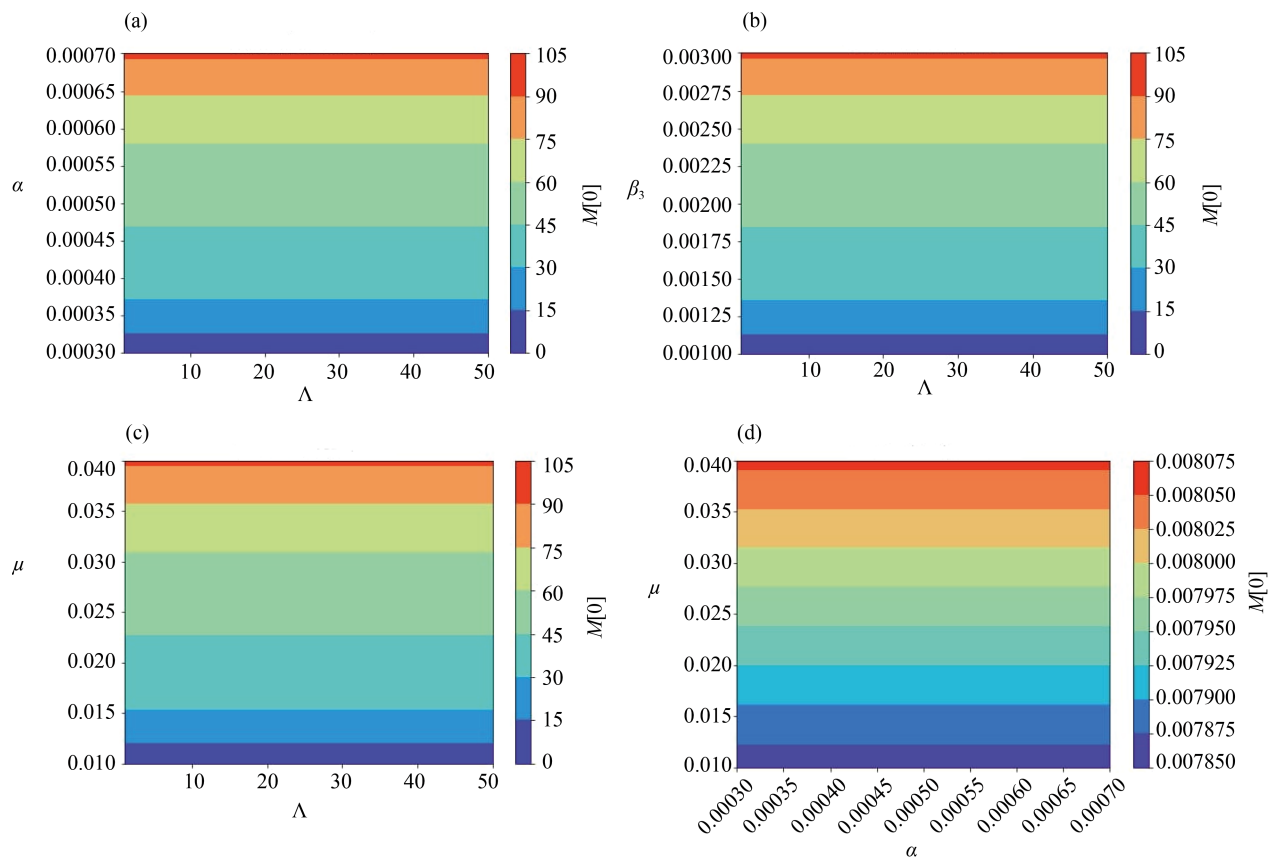


Figure 6. Contour plot representation with (a) Λ vs. α , (b) Λ vs. β_3 , (c) Λ vs. μ , (d) α vs. μ

Figure 7a shows a contour plot analyzing the intricate interplay between the rate of conditioning or purifying air and the rate at which cleanliness is lost, leading to its integration with the ambient air. Conversely, Figure 7b offers insight into the relationship between the rate of conditioning or purifying air and the rate at which cleanliness is lost, contributing to its integration with polluted air. Furthermore, Figure 7c provides a contour plot delving into the competitive dynamics between the rate of conditioning or purifying air and the natural removal rate of air from one spatial locale to another. Lastly, Figure 7d shows a contour plot scrutinizing the interaction between the rate of cleanliness loss and integration with general air and the natural removal rate of air between different locations.

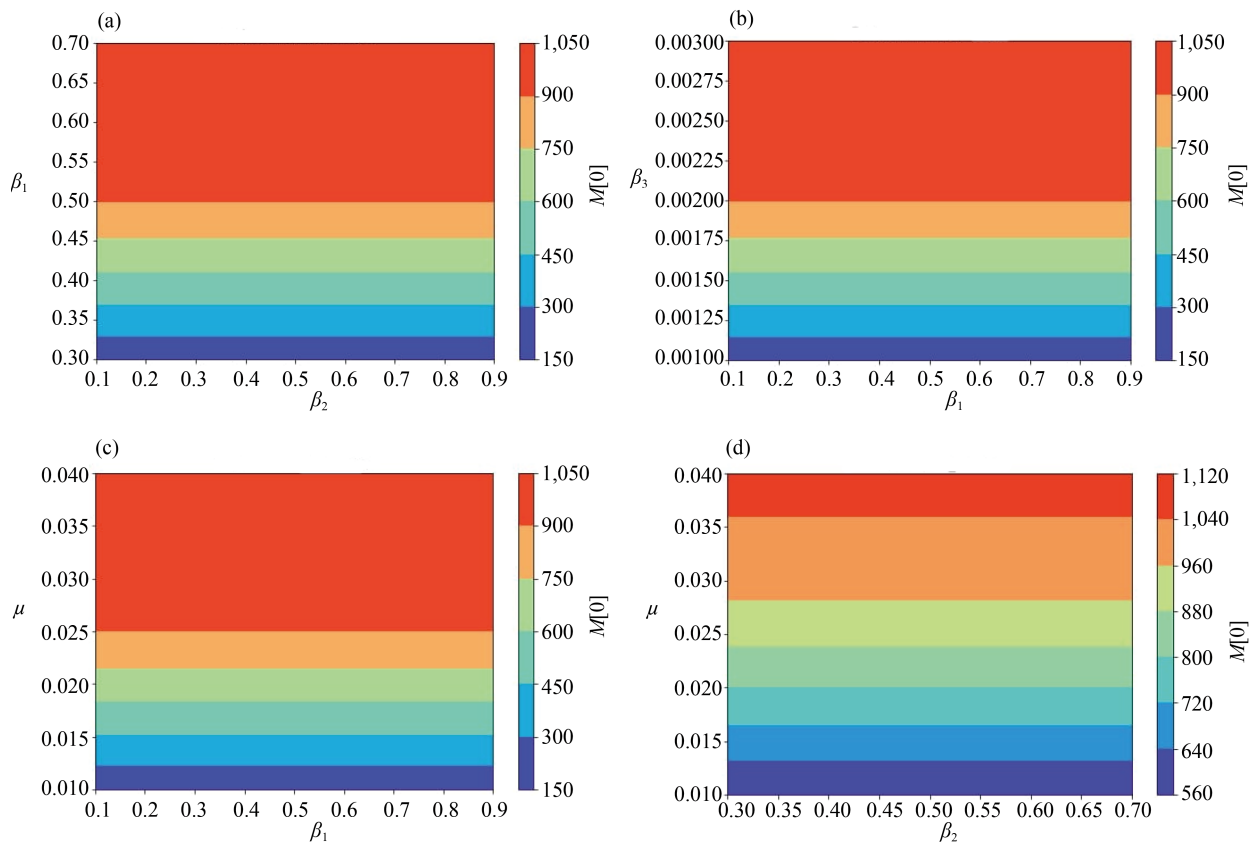


Figure 7. Contour plot representation (a) β_2 vs. β_1 , (b) β_1 vs. β_3 , (c) β_1 vs. μ , (d) β_2 vs. μ

6. Discussion

This paper undertakes the creation and evaluation of a model using deterministic ordinary differential equations to represent the dynamics of air conditioning. The primary focus is on exploring different equilibria within the model and systematically studying their stability, employing the Routh-Hurwitz criteria as a key analytical tool. Specifically, our investigation reveals that the pollution of the local asymptotic stability of free equilibrium is achieved when the fundamental reproduction number R_0 is smaller than 1, while it becomes unstable when R_0 exceeds 1. Notably, the endemic equilibrium only manifests when R_0 surpasses the critical threshold of 1. To validate and extend our analytical findings, numerical simulations are conducted across diverse sets of parameters. These simulations serve as a practical tool for observing the model's behavior under varying conditions. The outcomes of these simulations substantiate our theoretical results and provide valuable insights into the dynamic behavior of air pollution under different scenarios. In the broader context, our observations suggest that strategies for cleaning the air are effective not only in general air volumes but also in areas characterized by pollution. This underscores the importance of comprehensive approaches to air quality management that address both background pollution and localized sources. Furthermore, our research emphasizes the need for effective methodologies that not only clean the air but also ensure sustained maintenance over extended periods.

The collected results in this study offer significant insights into the dynamics of air pollution and the conditions necessary for its mitigation. The equilibrium analysis demonstrates that the system possesses two distinct steady states: the Pollution-Free Equilibrium (PFE), which is attainable when the basic reproduction number (R_0) remains below one, and the Endemic Equilibrium (EE), which persists when $R_0 > 1$. These findings provide a theoretical foundation for pollution control policies, indicating that sustained mitigation efforts are required to prevent pollution from becoming endemic. The stability analysis, established using the Routh-Hurwitz criteria, further reinforces these conclusions

by ensuring that the equilibria are mathematically robust, confirming the feasibility of maintaining a pollution-free environment under appropriate conditions. Additionally, numerical simulations, including phase portraits, 3D plots, and contour representations, validate the theoretical results and provide visual insights into air quality evolution under varying parameter conditions. These computational findings highlight the critical influence of key factors such as pollution recruitment (Λ), air purification rates (β_1), and environmental contamination (β_2, β_3) offering practical recommendations for policymakers. Notably, the results emphasize that reducing pollution sources, enhancing air cleaning mechanisms, and optimizing urban planning are the most effective strategies for keeping R_0 below the threshold for pollution-free stability. Overall, this research bridges the gap between theoretical modeling and real-world applications, providing a structured framework for understanding air pollution dynamics and guiding the development of sustainable environmental policies to improve air quality and public health outcomes.

Compared to existing air pollution models, such as statistical regression models or machine learning-based predictions, our approach offers a deeper mechanistic understanding of pollution dynamics. While empirical models can provide accurate short-term forecasts, they often lack interpretability and fail to capture the causal relationships governing pollution spread. On the other hand, some atmospheric dispersion models, such as the Gaussian plume model, focus on spatial pollution distribution rather than temporal evolution and equilibrium behavior. Our model bridges this gap by offering a dynamic, time-dependent analysis that incorporates both the evolution of pollution levels and their long-term stability properties. Moreover, models such as the Operational Street Pollution Model (OSPM) emphasize localized air pollution in urban areas due to traffic emissions, whereas our model takes a broader perspective, accounting for pollution interactions across different compartments of air quality. In a broader context, our findings suggest that strategies for improving air quality must be multifaceted, addressing both large-scale atmospheric pollution and localized sources of contamination. Our results emphasize that cleaning mechanisms targeting general air volumes are effective, but they must be complemented by interventions in high-pollution regions to prevent pollution resurgence. This underscores the necessity of developing comprehensive air pollution management strategies that integrate proactive reduction measures with long-term maintenance efforts. Furthermore, our research highlights the need for policies and practical measures that not only mitigate air pollution in the short term but also ensure its long-term control. By advancing our understanding of air pollution dynamics through this study, we provide a valuable foundation for policymakers, environmental scientists, and urban planners. The insights gained from our model can guide the design of efficient pollution control strategies, such as optimizing air filtration systems, regulating industrial emissions, and promoting sustainable urban planning.

This holistic perspective is crucial for developing strategies that contribute to long-term improvements in air quality. As we advance our understanding of air pollution dynamics through this research, we anticipate that our findings will inform policy and practice, contributing to the development of effective and sustainable solutions for mitigating the impact of air pollution.

7. Conclusions

This study presents a mathematical model to analyze air pollution dynamics, focusing on equilibrium conditions and stability analysis. The research introduces an Air Pollution Compartmental (APC) model that classifies air into general, polluted, and clean categories, allowing for a structured evaluation of pollution trends. Through theoretical derivations and numerical simulations, the study establishes conditions under which the system attains either a pollution-free equilibrium or an endemic equilibrium, with stability governed by the basic reproduction number R_0 . The results indicate that air pollution remains controlled when $R_0 < 1$, while pollution persists when $R_0 > 1$, emphasizing the importance of mitigation strategies. The study underscores the significance of air purification mechanisms and policy interventions in reducing pollution levels. Key recommendations include stricter emission controls, enhanced air filtration technologies, and urban planning strategies to improve natural ventilation. The theoretical findings are validated through numerical simulations, reinforcing the practical applicability of the model in environmental management. By bridging mathematical modeling with real-world environmental concerns, this research provides a robust framework for understanding air pollution

dynamics and guiding effective pollution control strategies. Future studies can extend this model by incorporating additional factors such as meteorological influences and spatial variability to enhance its predictive capabilities.

Conflicts of interest

The authors declare that there is no competing financial interest or personal relationship that could have appeared to influence the work reported in this paper.

References

- [1] Santhosh Kumar G, Gunasundari C, Boulaaras SM, Aakash M, Sharmila NB. Genetic differentiation of prey predator interaction model along with an Holling type-II functional response. *Partial Differential Equations in Applied Mathematics*. 2024; 9: 100649. Available from: <https://doi.org/10.1016/j.pdeam.2024.100649>.
- [2] Boulaaras S, Rashid J, Choucha A, Zarái A, Benzahi M. Blow-up and lifespan of solutions for elastic membrane equation with distributed delay and logarithmic nonlinearity. *Boundary Value Problems*. 2024; 36(1): 2024. Available from: <https://doi.org/10.1186/s13661-024-01834-4>.
- [3] Mohandoss A, Chandrasekar G, Meetei MZ, Msmali AH. Fractional order mathematical modelling of HFMD transmission via Caputo derivative. *Axioms*. 2024; 13(4): 213. Available from: <https://doi.org/10.3390/axioms13040213>.
- [4] Aakash M, Gunasundari C, Sabarinathan S, Boulaaras SM, Himaadan A. Mathematical insights into the SEIQRD model with Allee and fear dynamics in the context of COVID-19. *Partial Differential Equations in Applied Mathematics*. 2024; 11(6). Available from: <https://doi.org/10.1016/j.pdeam.2024.100012>.
- [5] Aakash M, Gunasundari C. Analysis of fractional order mathematical modelling of HFMD transmission through ABC derivative. *Mathematica Applicanda*. 2023; 51(2). Available from: <https://doi.org/10.1007/s40314-023-00556-5>.
- [6] Li Z, Ho KF, Lee HF, Yim SHL. Development of an integrated model framework for multi-air-pollutant exposure assessments in high-density cities. *Atmospheric Chemistry and Physics*. 2024; 24(1): 649-661. Available from: <https://doi.org/10.5194/acp-24-649-2024>.
- [7] Khamlich M, Stabile G, Rozza G, Környei L, Horváth Z. A physics-based reduced order model for urban air pollution prediction. *Computer Methods in Applied Mechanics and Engineering*. 2023; 417: 116416. Available from: <https://doi.org/10.1016/j.cma.2023.116416>.
- [8] Steinberga I, Sustere L, Bikseb J, Bikse JJ, Kleperisc J. Traffic induced air pollution modelling: Scenario analysis for air quality management in street canyon. *Procedia Computer Science*. 2018; 149: 384-389. Available from: <https://doi.org/10.1016/j.procs.2018.05.056>.
- [9] Santhosh Kumar G, Gunasundari C. Turing instability of a diffusive predator-prey model along with an Allee effect on a predator. *Communications in Mathematical Biology and Neuroscience*. 2022; 2022: 40. Available from: <https://doi.org/10.3934/cmb.2022.40>.
- [10] Pope CA III, Coleman N, Pond ZA, Burnett RT. Fine particulate air pollution and human mortality. *Journal of Environmental Research*. 2020; 191: 10997. Available from: <https://doi.org/10.1016/j.envres.2020.109997>.
- [11] Santhosh Kumar G, Gunasundari C. Dynamical analysis of two-preys and one predator interaction model with an Allee effect on predator. *Malaysian Journal of Mathematical Sciences*. 2022; 17(3): 263-281. Available from: <https://doi.org/10.11113/mjms.v17n3.1048>.
- [12] Krall JR, Keller JP, Peng RD. Assessing the health estimation capacity of air pollution exposure prediction models. *Environmental Health*. 2022; 21(1): 35. Available from: <https://doi.org/10.1186/s12940-022-00801-9>.
- [13] Ribeiro M. Air pollution models in epidemiologic studies with geostatistics and machine learning. *ArXiv:2211.09516*. 2022. Available from: <https://arxiv.org/abs/2211.09516> [Accessed 22 November 2022].
- [14] Han Y, Zhang Q, Li VO, Lam JC. Deep-AIR: A hybrid CNN-LSTM framework for air quality modeling in metropolitan cities. *ArXiv:2103.14587*. 2021. Available from: <https://arxiv.org/abs/2103.14587> [Accessed 15 March 2021].

- [15] van den Driessche P, Watmough J. Reproduction numbers and subthreshold endemic equilibria for compartmental models of disease transmission. *Mathematical Biosciences*. 2002; 180: 29-48. Available from: [https://doi.org/10.1016/S0025-5564\(02\)00136-1](https://doi.org/10.1016/S0025-5564(02)00136-1).
- [16] Mishra BK, Keshri AK, Rao YS, Mishra BK, Mahato B, Ayesha S, et al. COVID-19 created chaos across the globe: Three novel quarantine epidemic models. *Chaos, Solitons and Fractals*. 2020; 138: 109928. Available from: <https://doi.org/10.1016/j.chaos.2020.109928>.
- [17] Leong WC, Kelani RO, Ahmad Z. Prediction of air pollution index using support vector machine. *Journal of Environmental Chemical Engineering*. 2020; 8(3): 103208. Available from: <https://doi.org/10.1016/j.jece.2020.103208>.
- [18] Cooper WW, Hemphill H, Huang Z, Li S, Lelas V, Sullivan DW. Survey of mathematical programming models in air pollution management. *European Journal of Operational Research*. 1997; 9: 1-35. Available from: [https://doi.org/10.1016/S0377-2217\(97\)00177-8](https://doi.org/10.1016/S0377-2217(97)00177-8).